Macromolecules

pubs.acs.org/Macromolecules Article

Vitrimer-like Polyampholyte Networks: Toward Elevated Creep Resistance and Fast Dynamic Exchanges

Jean-Emile Potaufeux,[†] Romain Tavernier,[†] Jérémy Odent,*[,†] and Jean-Marie Raquez

Cite This: https://doi.org/10.1021/acs.macromol.4c00378 Read Online

ACCESS | Metrics & More | Article Recommendations | Supporting Information

ABSTRACT: Vitrimers represent dynamic polymer networks with unique viscoelastic behavior, combining the best attributes of thermosets and thermoplastics. In this work, we report the concept of polyampholyte physical networks that go far beyond the merits of vitrimer-like materials by combining elevated creep resistance and fast dynamic exchanges. By contrast with most vitrimeric systems requiring out-of-stoichiometric approaches or external catalysts, we simply design polyampholyte physical networks of charge-balanced ionic methacrylates via free radical copolymerization combining poly(ethylene glycol) methyl ether methacrylate (PEGMA). The high ion concentration (i.e., from 33 to 67 mol %) enabled the formation of a physical network containing ionic cross-links acting as both sacrificial and permanent bonds mitigated by the presence of neutral PEGMA. In addition to their vitrimer-like behavior demonstrated using thermomechanical and rheological tools, these physical networks show exceptionally short relaxation times and high creep resistance. Conceptually, these polyampholyte physical networks due to extensive dynamic ion exchange open the door to more circular vitrimer-like systems toward more sustainable plastic materials.

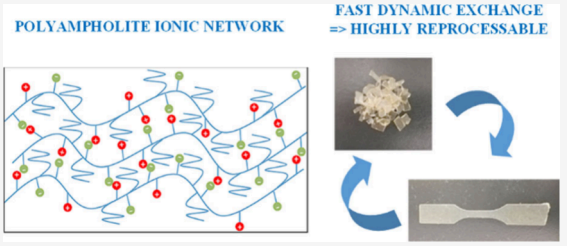

INTRODUCTION

The increasing demand toward sustainable and durable plastics from a circular approach has struggled researchers to improve the recyclability extent of thermoplastics or even to design reshapable and de facto recyclable thermosets.[1,2] Being permanently cross-linked, classical thermosets are insoluble, infusible, and nonprocessable, merely considering their post-consumer use as fillers after a grinding stage for low quality applications or their energetic conversion as end-life scenarios.[3] To increase the circularity of thermoset products, the introduction of reversible dynamic bonds into the polymer network is often reported as a solution to achieve melt-recyclable thermosets of maintained performances.[3] Although they still have poorly implemented in industry, this new class of thermosets can be achieved upon the introduction of dynamic covalent bonds that can break and reform in a perpetual manner upon an appropriate external trigger in a dissociative pathway[4,5] or can continuously endow bond exchange reactions in an associative pathway,[6,7] leading to covalent adaptable networks (CANs). For instance, purely dissociative networks such as Diels−Alder adducts undergo sol−gel phase transitions at specific transition temperatures, allowing their melt reprocessability.[8,9] The dissociative covalently bonded linkages are therein de facto broken before they are reconnected to another complementary moiety, leading to a dramatic on-demand viscosity drop upon thermal stimulation. However, the creep resistance is strongly depressed due to a reduction of the cross-linking density after reshaping.[9] As an alternative, Leibler et al. recently introduced the concept of vitrimers, whereby the associative mechanism of bond exchanges is based on transesterification reactions.[10] Currently, various strategies have been adopted to design *vitrimer* materials, including, e.g., transcarbamoylation, transcarbonation, transimination, and dioxaborolane transesterification.[10−14] Therein, the dissociation and reassociation of the associative covalently bonded linkages appear to occur *simultaneously*, maintaining a constant cross-linking density during the bond exchanges.[9] As a result, the viscosity does not dramatically decrease upon thermal stimulation, and the creep performance remains elevated, as opposed to dissociative dynamic covalent bonds. Given that the concept of vitrimers is coined to highlight an Arrhenius relationship between viscosity and temperature, the latter has initially been ascribed to associative CANs[13] and more recently extended to some dissociative CANs with thermomechanical properties close to vitrimers, for which the term "vitrimer-like" as sometimes been coined.[4,9,15] Thus, vitrimer-like materials are described as thermosetting networks that are able to flow following an Arrhenius temperature dependence but with chemistries that are not considered "associative". However, such CANs have not been able to meet the environmental challenges, particularly both elevated reprocessability and recyclability.

Received: February 15, 2024
Revised: July 24, 2024
Accepted: August 7, 2024

https://doi.org/10.1021/acs.macromol.4c00378
Macromolecules XXXX, XXX, XXX−XXX

Indeed, these vitrimers present a too slow bond exchange rate, restricting their implementation using classical melt-processing tools, such as extrusion technology. All in all, designing a system that combines sufficient mechanical integrity with the required very fast topology rearrangements (i.e., stress−relaxation and flow) generally involves the use of highly active catalysts for an improved recyclability.[11,16] More recently, strategies such as the use of covalently bonded catalysts, the incorporation of strongly bonded ionic moieties, and even catalyst-free reactions have been developed to make these materials more reprocessable.[11,17−19] For instance, transalkylation, as a covalent dynamic exchange reaction that generates charged structures, has shown to be useful for controlling the macroscopic flow properties[20,21] as well as enabling improved ionic conductivity.[22] Although these different strategies were successfully applied to make these CANs melt-processable, the final thermomechanical performances of the resulting networks remain unsatisfactory and inferior.[23,24] We must again highlight that most chemical exchanges applied so far to the field of vitrimers are characterized by low viscous flow activation energies, i.e., often below 100 kJ mol^{-1}.[21]

Identifying more robust alternatives to covalently bound CANs is therefore appealing by integrating strong bonds as well as weak bonds into polymeric networks that can provide both fast exchange reactions and mechanical strength. On this basis, neutral polyampholytes are interesting systems built around strong/weak bonds, leading to high toughness and self-healing at the same. To date, most polyampholyte systems reported in the literature are built around self-healable hydrogels obtained by copolymerizing a charge balanced amount of oppositely charged monomers at high concentration so that the polymer chains entangled to form gels. It results in the polyampholyte chains containing multiple ionic bonds distributed randomly upon both the intrachain and interchain of various ionic strength. Interestingly, the strong ionic bonds present within these interchain, stabilized by entanglements, act as permanent cross-linking, while the weak ionic bonds, both interchain and intrachain, serve as dynamic and reversible sacrificial bonds to dissipate energy. Thanks to these features, these polyampholyte hydrogels have revealed that their self-healing is due to the reforming of a dynamic weak bond while the healing follows an Arrhenius process.[25] A recent work reported the design of a self-healing strengthening elastomer by engineering kinetic stability within an ampholyte system that could display an Arrhenius evolution of its viscoelastic properties. However, the thermomechanical properties of these as-designed physically cross-linked networks changed with time uncontrollably due to the thermodynamic instability after several thermal treatments.[26] In this work and for the first time to our knowledge, we report that polyampholyte physical networks with only ionic interactions can encompass the merits of vitrimer-like materials, together with elevated melt processability. More particularly, we demonstrate that polyampholyte networks can readily encompass an Arrhenius relationship between viscosity and temperature in analogy to vitrimers, together with both elevated creep performance and melt processability. This is accomplished toward designing polyampholyte terpolymers by free radical copolymerization of neutral poly(ethylene glycol) methacrylate (PEGMA) with both charge-balanced cationic 2-(dimethylamino)ethyl methacrylate (DMAEMA) and anionic methacrylic acid (MAA). The resulting polyampholyte terpolymers leverage dynamic ionic bond interactions through the formation of inter- and intrachains, leading to a unique property profile that combines enhanced ion mobilities mitigated by the polar segment of PEGMA within these terpolymers as well as elevated thermomechanical properties. To demonstrate their very unique vitrimer-like behavior, terpolymers of various ion concentrations (i.e., from 33 to 67 mol %) were designed in order to form a physical network containing ionic cross-links, acting as both sacrificial and permanent bonds. Interestingly, the time−temperature superposition principle applied from frequency sweep measurements demonstrates for the first time a vitrimer-like behavior for these ionically modified networks. The Arrhenius fitting leads to high activation energies comparable to covalent adaptable networks, as reported in the case of vitrimers built upon associative mechanisms. In addition, stress−relaxation experiments evidence exceptionally short relaxation times together with excellent recycling performance using extrusion technology.

EXPERIMENTAL SECTION

Materials. Methacrylic acid (MAA, >99%, TCI, stabilized with hydroquinone monomethyl ether (MEHQ)), (2-dimethylaminoethyl) methacrylate (DMAEMA, >98%, Sigma-Aldrich, stabilized with MEHQ), poly(ethylene glycol) methyl ether methacrylate (PEGMA, 300 g mol^{-1}, Sigma-Aldrich, stabilized with MEHQ and butylated hydroxytoluene), methyl methacrylate (MMA, >98%, stabilized with MEHQ), azobis(isobutyronitrile) (AIBN, Molekula), Ludox HS30 colloidal silica (mean diameter 18 nm, Aldrich), 3-(hydroxysilyl)-1-propanesulfonic acid (SIT, 40 wt %, Gelest), sodium hydroxide solution (1 M, Aldrich), zinc chloride (VWR), ethyl acetate (EtOAc, VWR), *N*,*N*-dimethylformamide (DMF, >98%, VWR), tetrahydrofuran (THF, >99.8%), and *n*-hexane (>98%, VWR) were used without any further purification.

Syntheses and Preparation of Ionic Polymethacrylates (IPM_n). The polymers were synthesized according to previously reported method.[26,27] A total of 20 g containing PEGMA and an equimolar ratio of MAA and DMAEMA was introduced into a 250 mL round flask with 0.01 equiv of AIBN and 60 mL of EtOAc. Traces of water and oxygen were removed off by conditioning the glass flask and applying several freezing/defreezing cycles under nitrogen and vacuum. The polymerization was performed at 70 °C for 6 h under stirring and a nitrogen atmosphere. After polymerization the product was precipitated into *n*-hexane and recovered by filtration. Finally, the products were dried at 60 °C in a vacuum oven (10^{-2} to 10^{-3} mbar) to evaporate any solvent traces. The recovery yield was close to 100% for all of the samples. Materials were named IPM_n, where *n* corresponds to the molar fraction of both ionic monomers (i.e., MAA and DMAEMA) in Table S1. NMR spectroscopy was performed in deuterated chloroform for readily soluble polymers (IPM_{33} to IPM_{57}) and showed full conversion of the methacrylates as reported previously. Because of the broad dispersity, attribution could not be performed rigorously, but similar to what observed in the literature, on different block copolymers.[28,29]

Standard nonionic polymethacrylate, further called IPM_0, was synthesized using similar method and equivalents as IPM_{50} but where MAA was replaced by MMA.

The resulting IPM got shaped into films by compression molding at 110 °C using the following procedure: no pressure for 2 min followed by 3 degassing steps and 2 min under 10 bar.

Instrumentation. *Size-Exclusion Chromatography (SEC).* SEC was carried out on an Agilent 1200 apparatus in THF (containing 2 wt % of NEt_3). Samples in solution (1 mg mL^{-1}) were injected with a 1 mL min^{-1} flow rate at 35 °C in a precolumn PL gel 10 mm (50 × 7.5 mm^2) followed by two gradient columns PL gel 10 mm mixed-B (300 × 7.5 mm^2). Molecular weights and molecular weight distributions were calculated by reference to a relative calibration curve made of poly(methyl methacrylate) standards.

https://doi.org/10.1021/acs.macromol.4c00378
Macromolecules XXXX, XXX, XXX−XXX

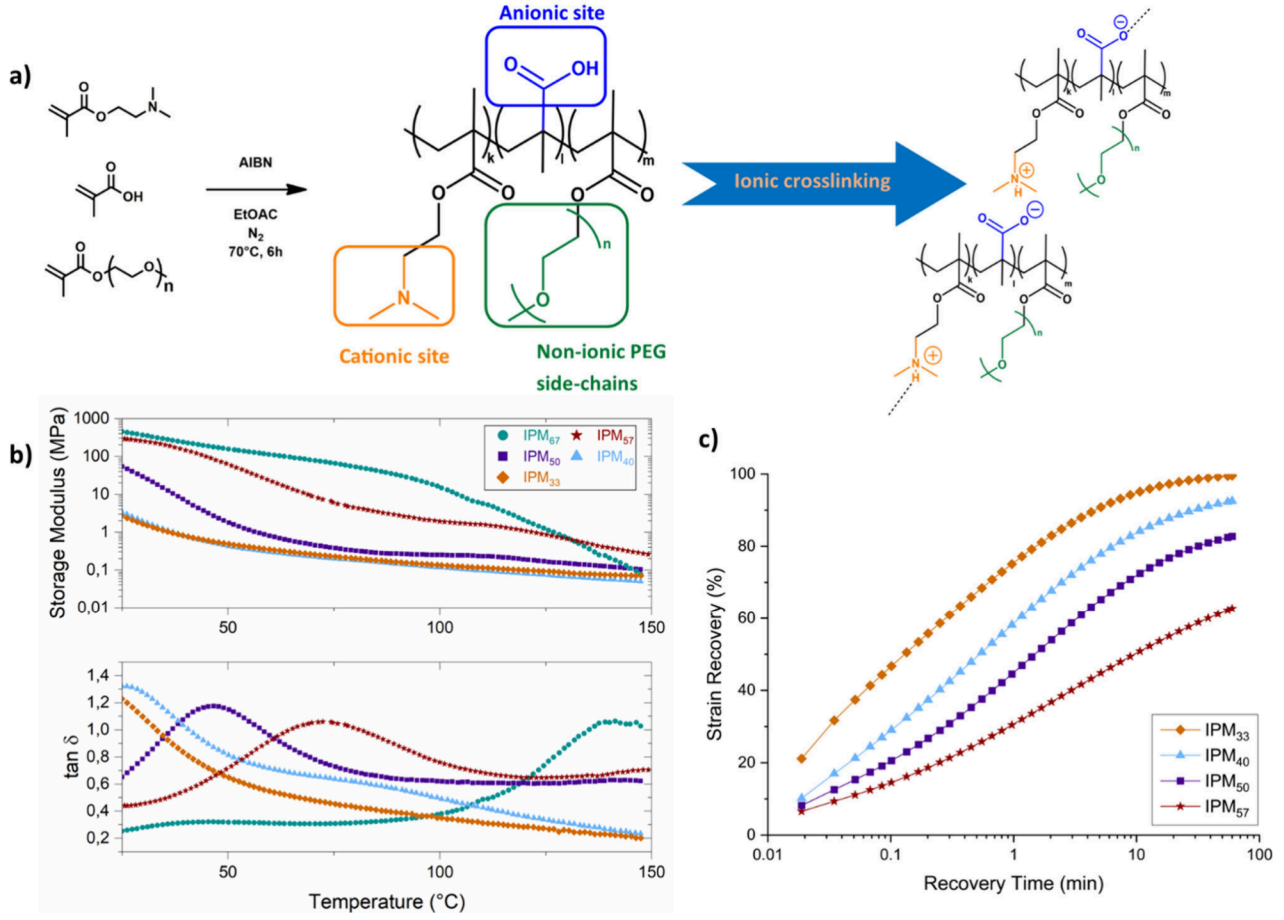

Figure 1. (a) Synthetic route of IPM_x of polyampholyte polymethacrylate containing cationic sites, anionic sites, and nonionic methacrylate residues and representation of its physically cross-linked network. (b) DMA thermomechanical properties with storage moduli of the networks containing different amounts of ionic moieties. (c) Strain recovery of different polyampholyte networks after stretching up to 100% at room temperature.

Fourier-Transform Infrared Spectroscopy (FTIR). FTIR spectra were recorded on an ATR-mode Bruker Tensor 27 spectrometer from 4000 to 600 cm^{-1} (spectral resolution of 1 cm^{-1}).

Proton Nuclear Magnetic Resonance Spectroscopy (NMR). NMR spectra were recorded in $CDCl_3$ using a Bruker Avance II-500.

Thermal Gravimetric Analysis (TGA). TGA was performed using a TGA Q500 from TA Instruments at a heating rate of 20 °C min^{-1} from room temperature to 800 °C under 25 mL min^{-1} nitrogen flow.

Dynamic Mechanical Thermal Analyses (DMTA). DMTA was performed under an ambient atmosphere using a DMTA Q800 apparatus from TA Instruments in tension film mode. The measurements were carried out at a constant frequency of 1 Hz, an amplitude of 20 μm, and a temperature range from 0 to 200 °C at a heating rate of 2 °C min^{-1}. Creep measurements were also performed at room temperature with a specific applied force depending on the sample for 5 min to reach a strain of approximately 100%, followed by 60 min of recovery after force release. Humidity-triggered shape memory was characterized at room temperature using the following four-step program: (1) deformation, the sample was elongated by applying a given load (stress ramp of 0.05 MPa/min until 0.1 MPa) at a relative humidity of 90%; (2) fixing, the sample was dried up to 5% of humidity under a constant load; (3) unloading, the load was removed within 3 min (at intervals of 0.05 MPa until 0 MPa); and (4) recovery, the humidity was increased up to 95% in a stepwise manner with a step interval of 10% lasting 60 min each time.

Tensile Tests. Tensile tests were carried out on a Zwick universal tensile testing machine (speed = 100 mm min^{-1}, preload = 1 N) according to ASTM D638 (with a length of reduced section of L_0 = 10 mm). The strain-rate dependency of polyampholytes was characterized through loading−unloading uniaxial cycles at 1, 10, and 100 mm min^{-1}.

Mechanistic Approach. Samples used for mechanistic testing were cut from compression-molded films into dog-bone specimens (ASTM D638). Loading−unloading uniaxial cycles were performed at room temperature by using an Instron E3000 electromagnetic tensile machine. A similar speed of 100 mm min^{-1} was used for loading and unloading steps with a maximum strain of 200%. A holding time of up to 10 min was imposed between loading and unloading steps.

Rheology. Rheology measurements were performed on an Anton Paar MCR302 rheometer using disk-shaped samples and plane geometries with diameter of 20 mm and a gap of 1 mm. Before running the rheological measurements, the disk-shaped samples were dried at 60 °C under reduced pressure (10^{-2} to 10^{-3} mbar) overnight. Amplitude sweep was performed from 0.01% to 100% of deformation. Time−temperature superposition (TTS) was also performed using measurements between 60 and 150 °C depending on the composition with a step of 10 °C on a frequency range from 100 to 0.1 Hz. Stress−relaxation experiments were also performed by following the same temperature program. A nominal force of 5 N was applied to every sample. Finally, creep tests were done at 20 °C around polymer's Tα with an applied pressure of 500 Pa for 10 min and a recovery of 20 min.

Methods. *Dissipated and Recovered Energy under Mechanical Testing.* Under tensile testing, the volume−energy of deformation, also called dissipated energy, is defined as eq 1:

$$E_{def} = \int_0^{\varepsilon_{break}} \sigma \, d(\varepsilon) \quad (1)$$

https://doi.org/10.1021/acs.macromol.4c00378
Macromolecules XXXX, XXX, XXX−XXX

where σ is the nominal stress and ε the nominal strain.

Time−Temperature Superposition (TTS). In order to obtain TTS mastercurves based on frequency-sweep rheology measurements, horizontal shift factors a_T were applied in order to overlap frequency-sweep data along the reference temperature (50 °C for IPM_{33}, IPM_{40} and IPM_{50}, 70 °C for IPM_{57}, and 130 °C for IPM_{67}). No vertical shift factors b_T were applied to the moduli here. The Arrhenius equation was then used to determine activation energies by fitting the evolution of a_T with the temperature (eq 2):

$$\ln(a_T) = \frac{E_a}{R}\left(\frac{1}{T} - \frac{1}{T_{ref}}\right) \quad (2)$$

where E_a is the activation energy, R the universal gas constant, T the temperature, and T_{ref} the reference temperature.

The Williams−Landel−Ferry C_1 and C_2 parameters were determined from eq 3 using a_T determined from TTS mastercurves. The values were then reinjected in eq 3 to obtain extrapolation of log a_T as a function of temperature, using the same reference temperatures as from mastercurves.

$$\log(a_T) = -\frac{C_1(T - T_{ref})}{C_2 + T - T_{ref}} \quad (3)$$

Thermal Recycling. First, a film made of IPM_{57} was prepared by solvent-casting in DMF after the full dissolution of the polymer and drying at 60 °C for 48 h. Dog bones were then cut, and tensile tests were performed at 10 mm min^{-1} according to the Tensile Tests section.

Then, IPM_{57} was cut into pellets and extruded using a Xplore twin-screw microcompounder (15 cm^3) at 110 °C for 4 min at 30 rpm under ambient atmosphere. The resulting material was shaped into a film of approximately 1 mm thickness by compression molding at 110 °C by using the previous procedure. Dog-bone specimens were cut from the film and characterized under tensile testing. This procedure was repeated three times in total.

RESULTS AND DISCUSSION

Polyampholyte terpolymers are synthesized by free radical copolymerization of neutral PEGMA with equimolar mixed cationic DMAEMA and anionic MAA using azobis-(isobutyronitrile) (AIBN) as thermal initiator (Figure 1a). The equimolar cationic−anionic portions within the resulting polyampholyte networks, so-called IPM_x, where IPM stands for ionic polymer material and where x, the molar fraction of mixed ionic counterparts, is equal to 0, 33, 40, 50, 57, and 67 mol %. Among them, IPM_0 matched with a standard nonionic PEGMA-based random copolymer integrating 50 mol % of neutral methyl methacrylate (MMA) counterpart. The resulting IPM_x presented relatively broad dispersity ($2 < Đ < 3.5$) and molecular weight (12 kg $mol^{-1} < M_n < 19$ kg mol^{-1}) (Table S1). The polymerization degree is limited both by protonation of the amine, happening immediately after dissolution in EtOAc, and by limited solubility of the formed network in the media. These observations are in line with previous literature.[26,27] Additionally, ^{1}H NMR spectroscopy shows broad signals for the polymers, with complete disparition of the monomer signals. A typical spectrum is displayed as Figure S1, and signals are observed according to the literature on different copolymers.[28,29] The high dispersity evidenced by SEC is also noticed by the overlapping of characteristic peaks of different comonomers. The role of polar PEGMA segment within the resulting ionic materials is to enable efficient ionic association−dissociation during the bond exchanges as well as to tune the mechanical performances of the resulting networks as reported elsewhere.[30−32] The ionic association extent is thereby determined by FTIR, whereby the appearance of a well-defined band at ca. 1560 cm^{-1} is assigned to the formation of carboxylates consistent with maximum Coulomb interactions between cationic DMAEMA and anionic MAA counterparts within IPM_x. This is highlighted by the comparison of both FTIR spectra of pure DMAEMA and MAA monomers, where this band does not appear, and their stoichiometric mixtures, where the band is present, as shown in Figure S2. All obtained networks FTIR spectra display the same 1560 cm^{-1} band in Figure S3.[33,34]

The presence of ionic interactions endows the materials with an unprecedented set of properties. For instance, the ionic motifs readily allow the fine-tuning of the overall mechanical performance, providing access to a range of behaviors from brittle to ductile (Figure S4). When IPM_{33} and IPM_{40} are soft and ductile materials (average $\varepsilon_b \sim 400\%$, $\sigma_y \sim 0.5$ MPa, and TT ~ 1 MJ m^{-3}, Table S2), IPM_{67} behaves as a stiff and brittle material (average $\varepsilon_b \sim 70\%$, $\sigma_y \sim 5$ MPa, and TT ~ 3.5 MJ m^{-3}, Table S2). Intermediate IPM_{50} and IPM_{57} likely display some combination of ductile and brittle behaviors with simultaneous improvements in stiffness, toughness, and elongation (average $\varepsilon_b \sim 600\%$, $\sigma_y \sim 5$ MPa, and TT ~ 23 MJ m^{-3}, Table S2). Additionally, solicitation at different speeds (1, 10, and 100 mm min^{-1}) with a stretching extent up to 250% shows that the material is capable to adapt to fast solicitations (Figure S5). While the overall mechanical performances of our ionic systems closely resemble to those of most CANs,[35,36] we attribute the mechanism by which the resulting ionic materials dissipate mechanical energy to the dissociation dynamics of temporary ionic cross-links present in the system.[37,38] DMTA further evidenced the improved thermomechanical performance relative to higher and broader α-transition temperatures (T_α) as the result of optimal ionic interactions in the system (Figure 1b and Table S2).[27] Overall, a ca. 100-fold increase in the storage modulus at ambient temperature is recorded by leveraging the dynamic and reversible nature of electrostatic interactions present in ionic systems. In addition, the wide range of T_α, ranging from ca. 20 °C for IPM_{33} to ca. 100−140 °C for IPM_{67}, attested that their thermomechanical properties be readily engineered by adequately varying the extent of these dynamic ionic cross-links within the material (see Table S2 and Figure 1b). These thermoset-like properties rely on physical cross-linking related to ions being associated altogether, as demonstrated by the previously discussed FTIR bands. These thermomechanical properties can be modulated by tuning the nature of ionic bonds, for instance, by adding a salt during the processing. When adding a divalent cation, Zn^{2+} (using $ZnCl_2$), in a slight excess compared to methacrylic acid content, we observe an important shift toward higher alpha transition temperatures by DMA, even if lower moduli are measured (Figure S6, T_α shifts from ca. 46 °C for IPM_{50} to ca. 116 °C for IPM_{50} + $ZnCl_2$). These differences reveal that different types of ionic clusters will change the mechanical properties, probably due to the different activation energy of ion dissociation. It also must be noted that the design of the polymers does not make the networks sensible to water, as evidenced by shape-memory experiments on IPM_{50} under controlled humidity, that did not evidence a dramatic effect of relative humidity (Figure S7). While thermogravimetric analyses show early weight loss, up to 6% at 100 °C for IPM_{67} (Figure S8), NMR spectroscopy did not reveal any free water signal (Figure S1). Combining TGA, humidity-controlled DMA, and NMR spectroscopy, we consider that the materials have a stable water content that

https://doi.org/10.1021/acs.macromol.4c00378
Macromolecules XXXX, XXX, XXX−XXX

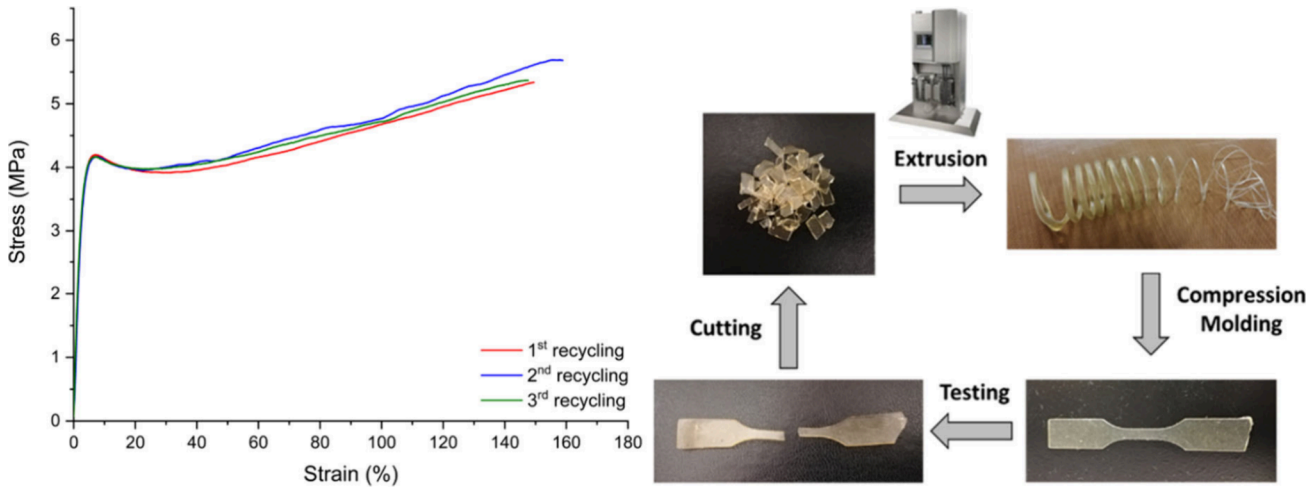

Figure 2. Recycling of IPM_{57} by an extrusion-assisted process and evaluation of the tensile properties of r-IPM_{57}.

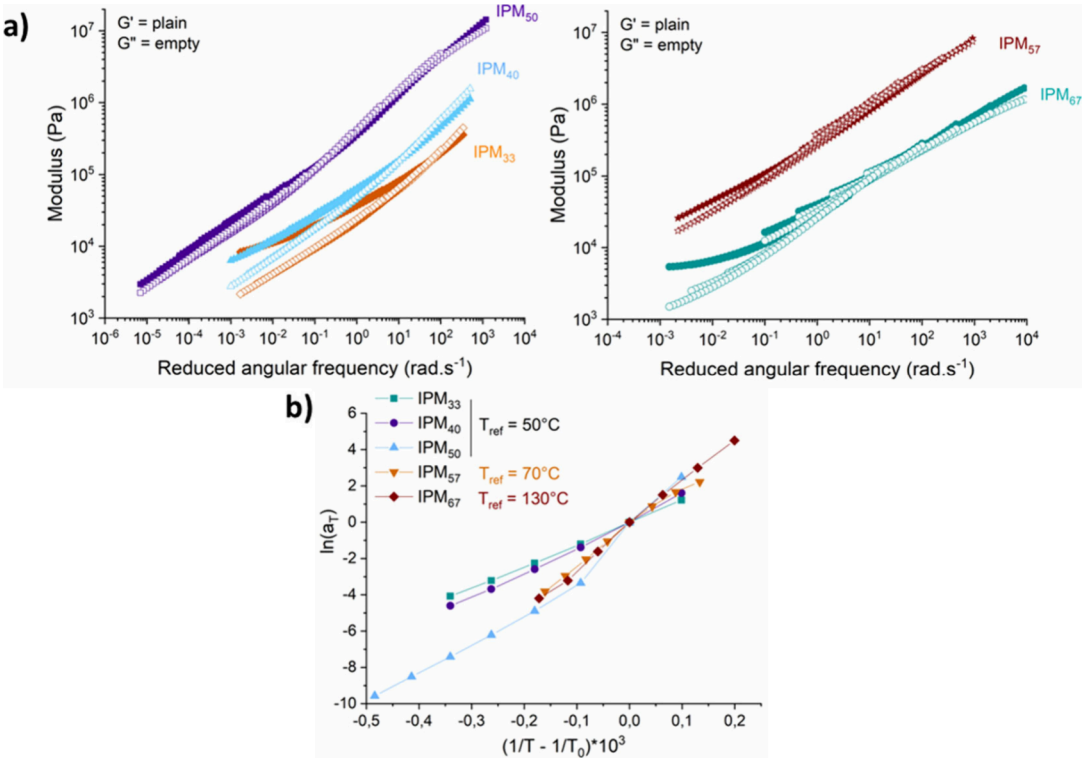

Figure 3. (a) Frequency-sweep mastercurves of IPM_x. For the sake of clarity, two figures are presented. (b) Arrhenius fitting of horizontal shift factors (a_T) of IPM_x.

is strongly linked in the network. Additionally, thermal stability of materials remains quite high, with a main degradation event happening mostly over 400 °C for all IPM_x. Consistent with the broad T_α, ensuring the suitable conditions for shape memory recovery, the resulting ionic materials not only sustain a very high level of strain but also exhibit self-recovery after extensive deformation. Though, the higher the ionic concentration within IPM_x, the lower the strain recovery, going from a complete strain recovery for IPM_{33} to partial recoveries in the range of ca. 90%, 80%, and 60% for IPM_{40}, IPM_{50}, and IPM_{57} (IPM_{67} does not sustain 100% strain), respectively (Figure 1c). Still, at least 50% of the strain recovery happens within 10 min at room temperature, consistent with moderate to high physical cross-linking densities, analogous to most rubbers.[35] Building on these dynamic ionic motifs, the ability of the resulting IPM_x to be reprocessed under mild conditions is evaluated (Figure 2). Therein, IPM_{57} is subjected to at least 3 reprocessing cycles involving the cutting and the reshaping through solvent-free extrusion at 110 °C, confirming the absence of any covalent cross-linking and the preservation of the mechanical integrity. Since dynamic polymer networks require *robust exchange reactions that proceed without any side-reactions for extended time* periods, we envisioned that the resulting ionic materials should outperform most CANs and vitrimer-like systems by allowing a simple and easy recycling process.

Although the resulting ionic materials are noncovalently cross-linked, leading to their full dissolution in, e.g., THF, a

https://doi.org/10.1021/acs.macromol.4c00378
Macromolecules XXXX, XXX, XXX−XXX

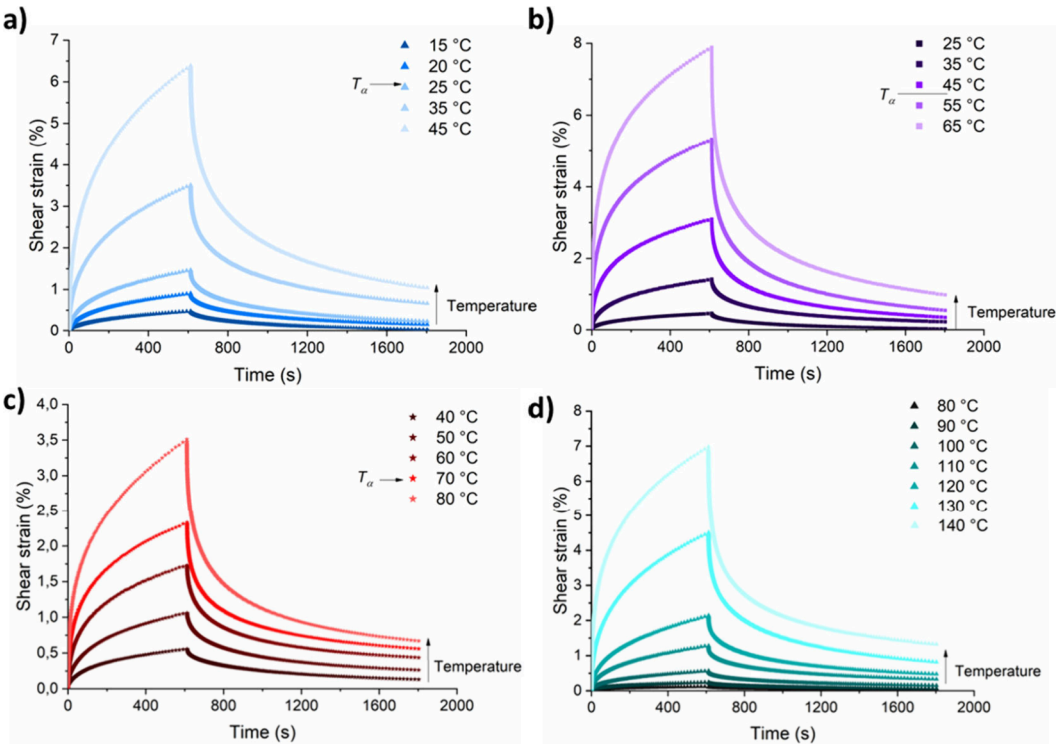

Figure 4. Creep and recovery behavior with a stress of 500 Pa of (a) IPM_{40}, (b) IPM_{50}, (c) IPM_{57}, and (d) IPM_{67}.

liquid-to-solid transition obviously occurs with the ionic concentration of IPM_x. Frequency sweep measurements using time−temperature superposition (TTS) readily allow rationalizing relaxation phenomena in resulting ionic materials around T_α (Figures S9−S13). While TTS often fails for dynamic polymer networks, including some ionic materials and vitrimers, because of structural changes or different temperature-dependent relaxation mechanisms,[39−41] polymers containing high amounts of ion-containing repeating units have shown to follow the TTS principle. For instance, polyelectrolyte complexes composed of associated polyanionic and polycationic strands follow both time−temperature and time−water superposition, or even time−salt superposition.[42,43] However, these examples relate to materials containing high water amounts. Nevertheless, our resulting IPM_x follows the TTS principle, suggesting the concomitant breaking and restoration of the dynamic ionic bonds (i.e., no chemical or physical changes involved) at different temperatures.[44] For the different ionic contents within IPM_x, we were able to construct mastercurves from frequency sweep measurements (Figure 3a) using different reference temperatures (i.e., 130 °C for IPM_{67}, 70 °C for IPM_{57}, and 50 °C for IPM_{33}, IPM_{40}, and IPM_{50}). We can observe from Figure 3a that no plateau occurs and that the rheological behaviors resemble that of thermoplastics with little to no entanglement. Reporting the evolution of horizontal shift factors a_T with the temperature demonstrates that these materials follow an Arrhenius law (Figure 3b), except for IPM_{50} which seems to display two different slopes, probably because the reference temperature is chosen close to the T_g for this specific network. The Arrhenius equation thereby revealed the dynamics of the resulting ionic materials and gives access to activation energy E_a, which is herein proportional to the energy required to break and reform ionic interactions, being representative of purely dissociative networks.[42] While the nonionic IPM_0 exhibits an activation energy of 80 kJ mol^{-1}, activation energies increase with the ionic concentration within IPM_x, ranging from 101 to 200 kJ mol^{-1} (Figure 3b and Figure S14). The resulting activation energy can be related to the energy barrier that is required to overcome the resistance to flow, which is herein thought to be proportional to the ionic bond dissociation energy.[42] Dissociative polymer networks usually display activation energies ranging from 40 to 160 kJ mol^{-1};[9,15,45] on the other hand, our IPM_x clearly present higher activation energies, revealing similar viscoelastic properties than most associative dynamic polymer networks (including CANs and vitrimers). Except for IPM_{50}, for which activation energy has been determined from the first slope, we can conclude from their rheological behavior that ion pairs dissociation and reassociation with fast kinetics still allow for the material to display viscosity evolution comparable to dynamic covalent networks.[11] Notably, the same activation energies can be obtained from the temperature dependence of gelation time (Figure S15). If the Arrhenius model seems to describe well the systems, the Williams−Landel−Ferry equation however does not fully capture the viscoelastic behavior of all the polymers. Figure S16 shows the extrapolation of the WLF model using the fitted C_1 and C_2 (Table S3) on log a_T, and larger deviations are observed for IPM_{57} and IPM_{67}. These results are expected since the range of measurements by rheology are on different windows around T_g for the materials. Because of the high alpha transition temperatures observed in high ionic content materials, measurements could not be done far over T_g.

In CANs or vitrimers, the E_a determined from stress−relaxation experiments is usually correlated to E_a of the corresponding bond exchange reaction on small molecules,[46] and the viscoelastic properties of ionic polymers are usually influenced by other parameters. For instance, the work of Chen et al. demonstrated that viscoelastic properties of ionomers could be predicted using the sticky Rouse model and from

https://doi.org/10.1021/acs.macromol.4c00378
Macromolecules XXXX, XXX, XXX−XXX

dielectric measurements.[47] In this work, the dissociation activation energy of a single ion could be determined (~58 kJ mol^{-1}), which is lower than the flow E_a of the ionomers (~150 kJ mol^{-1}). It means that the viscoelastic properties of ionomers are influenced by not only ion bond dissociation but also the association lifetime, the ion solvation, and the entanglements. The paper by Chen et al. also enlightens the effect of ion solvation specifically by comparing poly(ethylene oxide) (PEO)-based and poly(tetramethylene oxide) (PTMO)-based ionomers, highlighting that PEO facilitates ion dissociation with respect to good ion solvation as discussed earlier.

Creep experiments are performed to assess the materials flowing under static constraints (Figure 4a−d). While dynamic polymer networks typically suffer from poor creep resistance,[48−52] the creep tends to continuously increase as the temperature increases with respect to the constant rearrangement of the dynamic interactions.[49,53] Although the creep values of IPM$_x$ around T_α are broadly below 3% after 10 min when subjected to a 500 Pa load at their respective T_α, the creep increases but seems rather limited and remains below 8% beyond T_α. IPM$_x$ further display the ability to recover when the applied load is released, showing strain recovery capabilities from 65% for IPM$_{50}$ to 94% for IPM$_{40}$ after 20 min around T_α. As expected, the higher the temperature, the faster the strain recovery, thereby competing with most associative dynamic polymer networks (including CANs and vitrimers).[49,54,55] Stress−relaxation experiments around T_α are performed to assess the melt reprocessability of IPM$_x$ (Figures S17−S21). Therein, the complete relaxation of IPM$_x$ is observed with relaxation times (as determined at a 63%, i.e., 1/e, decrease of relaxation modulus) up to 0.1 s, which even decreases with temperature. Although the recorded stress−relaxation does not intimately satisfy the Arrhenius relationship (Figure S22), such very short relaxation times ultimately suggest ultrafast dynamic bond exchanges within the ionic system.

CONCLUSIONS

In the present work, polyampholyte physical networks that exhibit high mechanical performance together with excellent recycling ability are purposely designed. The mechanical properties of our IPM$_x$ are comparable to those of tough elastomers with high elongations at break. These polyampholyte materials showed a rheological behavior similar to vitrimers, thereby attesting that our networks can behave as associative systems. The obtained networks based on ionic dynamic exchanges showed good creep resistance, inferior to 5% around T_α under a 500 Pa load. They also showed a good creep recovery, with τ_{creep} between 200 and 600 s, depending on the quantity of ionic moieties. We also showed that these materials follow the TTS principle, after frequency-sweep measurements, highlighting that simple dynamic mechanisms govern the adaptability of the network, in contrast to most vitrimers where this principle does not usually apply. We can conclude that these unique features rely exclusively on ionic interactions. While activation energy is relatively high, leading to good mechanical integrity of the material, like a thermoset, very short relaxation times allowed an easy reprocessability. Hence, we are able to extrude and reshape a sample containing 57 mol % of ionic moieties 3 times without affecting its mechanical properties. Therefore, we can show a very unique set of thermomechanical properties that can be readily tuned upon the ionic loading within the IPM$_x$. The increase of ionic functions will lead to higher T_α, while a low loading will lead to elastomeric behavior and high elongations at break. We believe that ionic polymers could also play a role in more recyclable and sustainable plastics, showing that they can also compete with covalently cross-linked networks, thanks to rapid exchange between ionic cross-links, leading to an apparent associative exchange. This behavior of an ionic network has never been disclosed before, especially regarding the Arrhenius evolution of macroscopic flow, making our networks in competition with vitrimer or dissociative CANs that are able to retain a high cross-linking density. Usually, fast relaxation rates induce high creep, and it is difficult to find a good balance between mechanical integrity during polymer use and reprocessing ability. We believe that strong ionic interactions could also represent a very efficient tool to be used for the elaboration of highly recyclable polymers and plastics. Overall, the combination of high activation energies and short relaxation times readily endows the ionic materials with an unprecedented set of properties through a synergistic effect of a dissociative−associative mechanism.

ASSOCIATED CONTENT

Supporting Information

The Supporting Information is available free of charge at https://pubs.acs.org/doi/10.1021/acs.macromol.4c00378.

SEC data, NMR spectroscopy, FTIR of monomers and their mixture and of networks, stress−strain curves and data, TGA, frequency sweeps, TTS horizontal shift factors, gelation times, stress−relaxation experiments from rheology, creep experiments from DMTA, humidity-controlled DMA, additional stress−strain mechanical testing, DMA of selected samples with zinc salt modified formulation (PDF)

AUTHOR INFORMATION

Corresponding Author

Jérémy Odent − *Laboratory of Polymeric and Composite Materials (LPCM), Center of Innovation and Research in Materials and Polymers (CIRMAP), University of Mons (UMONS), 7000 Mons, Belgium;* orcid.org/0000-0002-3038-846X; Email: jeremy.odent@umons.ac.be

Authors

Jean-Emile Potaufeux − *Laboratory of Polymeric and Composite Materials (LPCM), Center of Innovation and Research in Materials and Polymers (CIRMAP), University of Mons (UMONS), 7000 Mons, Belgium*

Romain Tavernier − *Laboratory of Polymeric and Composite Materials (LPCM), Center of Innovation and Research in Materials and Polymers (CIRMAP), University of Mons (UMONS), 7000 Mons, Belgium;* orcid.org/0000-0001-8186-9557

Jean-Marie Raquez − *Laboratory of Polymeric and Composite Materials (LPCM), Center of Innovation and Research in Materials and Polymers (CIRMAP), University of Mons (UMONS), 7000 Mons, Belgium;* orcid.org/0000-0003-1940-7129

Complete contact information is available at: https://pubs.acs.org/10.1021/acs.macromol.4c00378

https://doi.org/10.1021/acs.macromol.4c00378
Macromolecules XXXX, XXX, XXX−XXX

Author Contributions

†J.-E.P., R.T., and J.O. contributed equally to this work.

Notes

The authors declare no competing financial interest.

■ ACKNOWLEDGMENTS

We gratefully acknowledge the support from the Wallonia and the European Commission "FSE and FEDER" for the research FEDER program entitled "UP_PLASTIC. J.-M.R. is a senior research associate at F.R.S.-F.N.R.S. (Belgium) and under the WEL-T research program entitled "CONSOLID". R.T. thanks Prof René Fulchiron and Dr Guillaume Sudre for fruitful discussions about rheology.

■ REFERENCES

(1) Fagnani, D. E.; Tami, J. L.; Copley, G.; Clemons, M. N.; Getzler, Y. D. Y. L.; McNeil, A. J. 100th Anniversary of Macromolecular Science Viewpoint: Redefining Sustainable Polymers. *ACS Macro Lett.* **2021**, *10* (1), 41−53.

(2) Moad, G.; Solomon, D. H. The Critical Importance of Adopting Whole-of-Life Strategies for Polymers and Plastics. *Sustainability* **2021**, *13* (15), 8218.

(3) Post, W.; Susa, A.; Blaauw, R.; Molenveld, K.; Knoop, R. J. I. A Review on the Potential and Limitations of Recyclable Thermosets for Structural Applications. *Polym. Rev.* **2020**, *60* (2), 359−388.

(4) Scheutz, G. M.; Lessard, J. J.; Sims, M. B.; Sumerlin, B. S. Adaptable Crosslinks in Polymeric Materials: Resolving the Intersection of Thermoplastics and Thermosets. *J. Am. Chem. Soc.* **2019**, *141* (41), 16181−16196.

(5) Kloxin, C. J.; Scott, T. F.; Adzima, B. J.; Bowman, C. N. Covalent Adaptable Networks (CANs): A Unique Paradigm in Cross-Linked Polymers. *Macromolecules* **2010**, *43* (6), 2643−2653.

(6) Zheng, N.; Xu, Y.; Zhao, Q.; Xie, T. Dynamic Covalent Polymer Networks: A Molecular Platform for Designing Functions beyond Chemical Recycling and Self-Healing. *Chem. Rev.* **2021**, *121* (3), 1716−1745.

(7) Imbernon, L.; Norvez, S. From Landfilling to Vitrimer Chemistry in Rubber Life Cycle. *Eur. Polym. J.* **2016**, *82*, 347−376.

(8) Adzima, B. J.; Aguirre, H. A.; Kloxin, C. J.; Scott, T. F.; Bowman, C. N. Rheological and Chemical Analysis of Reverse Gelation in a Covalently Cross-Linked Diels−Alder Polymer Network. *Macromolecules* **2008**, *41* (23), 9112−9117.

(9) Elling, B. R.; Dichtel, W. R. Reprocessable Cross-Linked Polymer Networks: Are Associative Exchange Mechanisms Desirable? *ACS Cent. Sci.* **2020**, *6* (9), 1488−1496.

(10) Montarnal, D.; Capelot, M.; Tournilhac, F.; Leibler, L. Silica-Like Malleable Materials from Permanent Organic Networks. *Science* **2011**, *334* (6058), 965−968.

(11) Cuminet, F.; Caillol, S.; Dantras, É.; Leclerc, É.; Ladmiral, V. Neighboring Group Participation and Internal Catalysis Effects on Exchangeable Covalent Bonds: Application to the Thriving Field of Vitrimer Chemistry. *Macromolecules* **2021**, *54* (9), 3927−3961.

(12) Guerre, M.; Taplan, C.; Winne, J. M.; Du Prez, F. E. Vitrimers: Directing Chemical Reactivity to Control Material Properties. *Chem. Sci.* **2020**, *11* (19), 4855−4870.

(13) Winne, J. M.; Leibler, L.; Du Prez, F. E. Dynamic Covalent Chemistry in Polymer Networks: A Mechanistic Perspective. *Polym. Chem.* **2019**, *10* (45), 6091−6108.

(14) Krishnakumar, B.; Sanka, R. V. S. P.; Binder, W. H.; Parthasarthy, V.; Rana, S.; Karak, N. Vitrimers: Associative Dynamic Covalent Adaptive Networks in Thermoset Polymers. *Chem. Eng. J.* **2020**, *385*, No. 123820.

(15) Chakma, P.; Morley, C. N.; Sparks, J. L.; Konkolewicz, D. Exploring How Vitrimer-like Properties Can Be Achieved from Dissociative Exchange in Anilinium Salts. *Macromolecules* **2020**, *53* (4), 1233−1244.

(16) Zhang, B.; De Alwis Watuthanthrige, N.; Wanasinghe, S. V.; Averick, S.; Konkolewicz, D. Complementary Dynamic Chemistries for Multifunctional Polymeric Materials. *Adv. Funct. Materials* **2022**, *32* (8), No. 2108431.

(17) Hayashi, M.; Obara, H.; Miwa, Y. Design and Basic Properties of Polyester Vitrimers Combined with an Ionomer Concept. *Mol. Syst. Des. Eng.* **2021**, *6* (3), 234−241.

(18) Niu, X.; Wang, F.; Kui, X.; Zhang, R.; Wang, X.; Li, X.; Chen, T.; Sun, P.; Shi, A.-C. Dual Cross-Linked Vinyl Vitrimer with Efficient Self-Catalysis Achieving Triple-Shape-Memory Properties. *Macromol. Rapid Commun.* **2019**, *40* (19), No. 1900313.

(19) Niu, X.; Wang, F.; Li, X.; Zhang, R.; Wu, Q.; Sun, P. Using Zn2+ Ionomer To Catalyze Transesterification Reaction in Epoxy Vitrimer. *Ind. Eng. Chem. Res.* **2019**, *58* (14), 5698−5706.

(20) Jourdain, A.; Asbai, R.; Anaya, O.; Chehimi, M. M.; Drockenmuller, E.; Montarnal, D. Rheological Properties of Covalent Adaptable Networks with 1,2,3-Triazolium Cross-Links: The Missing Link between Vitrimers and Dissociative Networks. *Macromolecules* **2020**, *53* (6), 1884−1900.

(21) Obadia, M. M.; Jourdain, A.; Cassagnau, P.; Montarnal, D.; Drockenmuller, E. Tuning the Viscosity Profile of Ionic Vitrimers Incorporating 1,2,3-Triazolium Cross-Links. *Adv. Funct. Mater.* **2017**, *27* (45), No. 1703258.

(22) Lopez, G.; Granado, L.; Coquil, G.; Lárez-Sosa, A.; Louvain, N.; Améduri, B. Perfluoropolyether (PFPE)-Based Vitrimers with Ionic Conductivity. *Macromolecules* **2019**, *52* (5), 2148−2155.

(23) Hubbard, A. M.; Ren, Y.; Sarvestani, A.; Konkolewicz, D.; Picu, C. R.; Roy, A. K.; Varshney, V.; Nepal, D. Recyclability of Vitrimer Materials: Impact of Catalyst and Processing Conditions. *ACS Omega* **2022**, *7* (33), 29125−29134.

(24) Li, H.; Zhang, B.; Yu, K.; Yuan, C.; Zhou, C.; Dunn, M. L.; Qi, H. J.; Shi, Q.; Wei, Q.-H.; Liu, J.; Ge, Q. Influence of Treating Parameters on Thermomechanical Properties of Recycled Epoxy-Acid Vitrimers. *Soft Matter* **2020**, *16* (6), 1668−1677.

(25) Ihsan, A. B.; Sun, T. L.; Kurokawa, T.; Karobi, S. N.; Nakajima, T.; Nonoyama, T.; Roy, C. K.; Luo, F.; Gong, J. P. Self-Healing Behaviors of Tough Polyampholyte Hydrogels. *Macromolecules* **2016**, *49* (11), 4245−4252.

(26) Peng, Y.; Hou, Y.; Wu, Q.; Ran, Q.; Huang, G.; Wu, J. Thermal and Mechanical Activation of Dynamically Stable Ionic Interaction toward Self-Healing Strengthening Elastomers. *Mater. Horiz.* **2021**, *8* (9), 2553−2561.

(27) Peng, Y.; Zhao, L.; Yang, C.; Yang, Y.; Song, C.; Wu, Q.; Huang, G.; Wu, J. Super Tough and Strong Self-Healing Elastomers Based on Polyampholytes. *J. Mater. Chem. A* **2018**, *6* (39), 19066−19074.

(28) De Jesús-Téllez, M. A.; Sánchez-Cerrillo, D. M.; Quintana-Owen, P.; Schubert, U. S.; Contreras-López, D.; Guerrero-Sánchez, C. Kinetic Investigations of Quaternization Reactions of Poly[2-(Dimethylamino)Ethyl Methacrylate] with Diverse Alkyl Halides. *Macromol. Chem. Phys.* **2020**, *221* (9), No. 1900543.

(29) Vardaxi, A.; Pispas, S. Stimuli-Responsive Self-Assembly of Poly(2-(Dimethylamino)Ethyl Methacrylate-Co-(Oligo Ethylene Glycol)Methacrylate) Random Copolymers and Their Modified Derivatives. *Polymers* **2023**, *15* (6), 1519.

(30) Tu, J.; Li, H.; Cai, Z.; Zhang, J.; Hu, X.; Huang, J.; Xiong, C.; Jiang, M.; Huang, L. Phase Change-Induced Tunable Dielectric Permittivity of Poly(Vinylidene Fluoride)/Polyethylene Glycol/Graphene Oxide Composites. *Composites Part B: Engineering* **2019**, *173*, No. 106920.

(31) Guo, Z.; Zhang, Y.; Dong, Y.; Li, J.; Li, S.; Shao, P.; Feng, X.; Wang, B. Fast Ion Transport Pathway Provided by Polyethylene Glycol Confined in Covalent Organic Frameworks. *J. Am. Chem. Soc.* **2019**, *141* (5), 1923−1927.

(32) Xue, Z.; He, D.; Xie, X. Poly(Ethylene Oxide)-Based Electrolytes for Lithium-Ion Batteries. *J. Mater. Chem. A* **2015**, *3* (38), 19218−19253.

https://doi.org/10.1021/acs.macromol.4c00378
Macromolecules XXXX, XXX, XXX−XXX

(33) Zeng, Z.; Wang, S.; Yang, S. Synthesis and Characterization of PbS Nanocrystallites in Random Copolymer Ionomers. *Chem. Mater.* **1999**, *11* (11), 3365−3369.
(34) Demarger-Andre, S.; Domard, A. Chitosan Carboxylic Acid Salts in Solution and in the Solid State. *Carbohydr. Polym.* **1994**, *23* (3), 211−219.
(35) Cao, L.; Fan, J.; Huang, J.; Chen, Y. A Robust and Stretchable Cross-Linked Rubber Network with Recyclable and Self-Healable Capabilities Based on Dynamic Covalent Bonds. *J. Mater. Chem. A* **2019**, *7* (9), 4922−4933.
(36) Yue, L.; Bonab, V. S.; Yuan, D.; Patel, A.; Karimkhani, V.; Manas-Zloczower, I. Vitrimerization: A Novel Concept to Reprocess and Recycle Thermoset Waste via Dynamic Chemistry. *Global Challenges* **2019**, *3* (7), 1800076.
(37) Mayumi, K.; Marcellan, A.; Ducouret, G.; Creton, C.; Narita, T. Stress−Strain Relationship of Highly Stretchable Dual Cross-Link Gels: Separability of Strain and Time Effect. *ACS Macro Lett.* **2013**, *2* (12), 1065−1068.
(38) Long, R.; Mayumi, K.; Creton, C.; Narita, T.; Hui, C.-Y. Time Dependent Behavior of a Dual Cross-Link Self-Healing Gel: Theory and Experiments. *Macromolecules* **2014**, *47* (20), 7243−7250.
(39) Ricarte, R. G.; Shanbhag, S. Unentangled Vitrimer Melts: Interplay between Chain Relaxation and Cross-Link Exchange Controls Linear Rheology. *Macromolecules* **2021**, *54* (7), 3304−3320.
(40) Sun, T. L.; Luo, F.; Hong, W.; Cui, K.; Huang, Y.; Zhang, H. J.; King, D. R.; Kurokawa, T.; Nakajima, T.; Gong, J. P. Bulk Energy Dissipation Mechanism for the Fracture of Tough and Self-Healing Hydrogels. *Macromolecules* **2017**, *50* (7), 2923−2931.
(41) Ling, G. H.; Wang, Y.; Weiss, R. A. Linear Viscoelastic and Uniaxial Extensional Rheology of Alkali Metal Neutralized Sulfonated Oligostyrene Ionomer Melts. *Macromolecules* **2012**, *45* (1), 481−490.
(42) Suarez-Martinez, P. C.; Batys, P.; Sammalkorpi, M.; Lutkenhaus, J. L. Time−Temperature and Time−Water Superposition Principles Applied to Poly(Allylamine)/Poly(Acrylic Acid) Complexes. *Macromolecules* **2019**, *52* (8), 3066−3074.
(43) Ali, S.; Prabhu, V. Relaxation Behavior by Time-Salt and Time-Temperature Superpositions of Polyelectrolyte Complexes from Coacervate to Precipitate. *Gels* **2018**, *4* (1), 11.
(44) Perego, A.; Lazarenko, D.; Cloitre, M.; Khabaz, F. Microscopic Dynamics and Viscoelasticity of Vitrimers. *Macromolecules* **2022**, *55* (17), 7605−7613.
(45) Bakkali-Hassani, C.; Berne, D.; Ladmiral, V.; Caillol, S. Transcarbamoylation in Polyurethanes: Underestimated Exchange Reactions? *Macromolecules* **2022**, *55*, 7974.
(46) Marco-Dufort, B.; Iten, R.; Tibbitt, M. W. Linking Molecular Behavior to Macroscopic Properties in Ideal Dynamic Covalent Networks. *J. Am. Chem. Soc.* **2020**, *142* (36), 15371−15385.
(47) Chen, Q.; Tudryn, G. J.; Colby, R. H. Ionomer Dynamics and the Sticky Rouse Model. *J. Rheol.* **2013**, *57* (5), 1441−1462.
(48) Spiesschaert, Y.; Guerre, M.; Imbernon, L.; Winne, J. M.; Du Prez, F. Filler Reinforced Polydimethylsiloxane-Based Vitrimers. *Polymer* **2019**, *172*, 239−246.
(49) Van Lijsebetten, F.; Debsharma, T.; Winne, J. M.; Du Prez, F. E. A Highly Dynamic Covalent Polymer Network without Creep: Mission Impossible? *Angew. Chem. Int. Ed* **2022**, *61*, e202210405.
(50) Meng, F.; Saed, M. O.; Terentjev, E. M. Rheology of Vitrimers. *Nat. Commun.* **2022**, *13* (1), 5753.
(51) Creton, C. 50th Anniversary Perspective: Networks and Gels: Soft but Dynamic and Tough. *Macromolecules* **2017**, *50* (21), 8297−8316.
(52) Si, P.; Jiang, F.; Cheng, Q. S.; Rivers, G.; Xie, H.; Kyaw, A. K. K.; Zhao, B. Triple Non-Covalent Dynamic Interactions Enabled a Tough and Rapid Room Temperature Self-Healing Elastomer for next-Generation Soft Antennas. *J. Mater. Chem. A* **2020**, *8* (47), 25073−25084.
(53) Perego, A.; Khabaz, F. Creep and Recovery Behavior of Vitrimers with Fast Bond Exchange Rate. *Macromol. Rapid Commun.* **2023**, *44*, 2200313.
(54) Denissen, W.; Winne, J. M.; Du Prez, F. E. Vitrimers: Permanent Organic Networks with Glass-like Fluidity. *Chem. Sci.* **2016**, *7* (1), 30−38.
(55) Li, L.; Chen, X.; Jin, K.; Torkelson, J. M. Vitrimers Designed Both To Strongly Suppress Creep and To Recover Original Cross-Link Density after Reprocessing: Quantitative Theory and Experiments. *Macromolecules* **2018**, *51* (15), 5537−5546.

https://doi.org/10.1021/acs.macromol.4c00378
Macromolecules XXXX, XXX, XXX−XXX